Entanglement-induced sub-Planck phase-space structures

Jitesh R. Bhatt,* Prasanta K. Panigrahi,† and Manan Vyas‡
Physical Research Laboratory, Navrangpura, Ahmedabad 380 009, India

(Received 20 April 2007; revised manuscript received 13 June 2008; published 10 September 2008)

We show that entanglement of two superposed coherent states produces sub-Planck structures in phase space. The origin of these structures depends entirely on entanglement, unlike those in Zurek [Nature (London) **412**, 712 (2001)], where the effect of entanglement was not considered. The constituent states are sensitive enough to carry out the Heisenberg sensitive measurements. However, their usefulness is limited in providing high sensitivity in either the position (x) direction or in the momentum (p) direction of the phase-space. Interestingly, the entanglement causes the proposed states to be sensitive in both x and p directions. This state offers a better sensitivity compared to the single partite compass state in Zurek [Nature (London) **412**, 712 (2001)] in carrying out precision measurements. It is also argued that such states are easy to create and are better suited for carrying out precision measurements.

DOI: 10.1103/PhysRevA.78.034101 PACS number(s): 03.65.Ud, 03.65.Ta

Recently, it has been demonstrated that the quantum states obtained from superposition of coherent states can be useful in quantum metrology, especially in carrying out Heisenberg-limited measurements and quantum parameter estimation [1,2]. Zurek showed that nonlocal superposition of coherent quantum states can have well-defined oscillatory structures in the phase space, at scales smaller than the Planck constant $\hbar$. More surprisingly, contrary to the commonly held belief, these structures can be physically important. The Wigner distribution function for a compass state $|\alpha\rangle+|-\alpha\rangle+|i\alpha\rangle+|-i\alpha\rangle$ has a checkerboard type of structure in phase space due to quantum interference. Here α is a complex parameter used for characterizing the coherent states and its magnitude signifies a distance from the origin in the phase space. The typical area a of the fundamental tile of the checkerboard is $a=\hbar\hbar/\mathcal{A}$, where $\mathcal{A}$ is the area of the accessible phase space, which can be estimated from the total energy. The sub-Planck structures arise because, for a compass state with superposition of well-separated coherent states in phase space, $\hbar/\mathcal{A}\ll 1$ and thus $a\ll\hbar$. The locations of the coherent states in the phase space of the compass state can be denoted by the intuitively obvious geographical notations, namely, north (N), south (S), east (E), and west (W), to denote their relative positions in phase space. It can be shown that the interference between the $NS(|i\alpha\rangle+|-i\alpha\rangle)$ and $EW(|-\alpha\rangle+|\alpha\rangle)$ combinations produces the checkerboard type of pattern [1]. If an act of measurement or any other process displaces the original compass state by a distance $\sqrt{a}$ in phase space, the sub-Planck structures allow the resultant state to be distinguished from the old one. These states are useful in carrying out Heisenberg-limited sensitive measurements [2]. It ought to be noted here that a simpler state involving just two superposed coherent states can also be used for this purpose. However, such states offer sensitivity only along the direction perpendicular to the line joining the two coherent states [2]. In comparison Zurek's compass state [1] can offer sensitivity in all directions of phase space albeit with half the accuracy for the same value of α.

The sub-Planck structures have been studied by various researchers to further investigate their properties and test some of the assumptions made. The issue of sensitivity to external perturbation of these structures, as the system evolves with time, was studied using Loschmidt echoes [3]. However, the results of this work remain inconclusive. Recently it has been demonstrated that the above compass states, due to their Heisenberg-limited sensitivity to external perturbation, can be utilized for quantum parameter estimation [2]. In this work, the state was entangled with a two-level atomic system for carrying out the measurements. Generation of the compass state in cavity QED and its decoherence characteristics were studied in Ref. [4]. Such states can also be generated during the fractional revival process of molecular wave packets [5]. A classical analog of these states was found in Ref. [6]. It was shown that two pulses displaced by a small sub-Fourier shift of the carrier frequency become mutually orthogonal. The single-particle compass state used in Ref. [1] is composed of four coherently superposed localized Gaussians. These states are rather difficult to produce. It was shown in Ref. [4] that the interference pattern (sub-Planckian structures) arising due to the superposition of all four Gaussians (NS and EW combinations) can disappear faster than the interference pattern between any two Gaussians due to decoherence. In this work, we aim to study the sub-Planck structures in the phase space of a bipartite system and analyze the role of entanglement in it. For this goal, we propose a new compass state $|\psi\rangle_c$:

$$|\psi\rangle_c = \frac{1}{\sqrt{2}}(A|\pm\alpha\rangle_1|\pm\iota\alpha\rangle_2 + B|\pm\iota\alpha\rangle_1|\pm\alpha\rangle_2), \quad (1)$$

where $A=A_1+iA_2$ and $B=B_1+iB_2$ are complex parameters that control the entanglement. The states in Eq. (1) are given by

$$|\pm\alpha\rangle = \frac{1}{\sqrt{2}}(|\alpha\rangle + |-\alpha\rangle). \quad (2)$$

The choice of the compass state $|\psi\rangle_c$ is such that, when

*jeet@prl.res.in
†prasanta@prl.res.in
‡manan@prl.res.in

one considers the Wigner function for a constituent particle state [i.e., for state like in Eq. (1)], it does not show any checkerboard pattern. But the Wigner function for the entire $|\psi\rangle_c$ shows these structures. It can be demonstrated that they arise solely due to entanglement. Since the degree of entanglement in the state given by Eq. (1) is determined by A and B only and does not depend on α, there are two different decoherence characteristics for the superposition and the entanglement. Superposition of the coherent state is strongly affected by noise processes, say absorption of photons, while it can have no effect on the entanglement [7]. The entangled coherent states are more robust against the decoherence arising due to photon absorption noise. Thus, keeping in mind the results of Refs. [4,7], the state proposed by us might be more suitable for carrying out Heisenberg-limited measurements. Since the proposed entangled states give sub-Planck structures in the Wigner function, they offer sensitivity in all directions in phase space.

We represent these states by localized coherent Gaussian states, to construct the normalized coordinate $|\pm\alpha\rangle \rightarrow \psi(x)$ and the momentum even states $|\pm i\alpha\rangle \rightarrow \varphi(x)$:

$$\psi(x) = \frac{e^{-(x+x_0)^2/2\delta^2} + e^{-(x-x_0)^2/2\delta^2}}{\sqrt{2}\pi^{1/4}\delta^{1/2}(1+e^{-x_0^2/\delta^2})^{1/2}} \tag{3}$$

and

$$\varphi(x) = \frac{e^{-x^2/2\delta^2+ip_0x/\hbar} + e^{-x^2/2\delta^2-ip_0x/\hbar}}{\sqrt{2}\pi^{1/4}\delta^{1/2}(1+e^{-p_0^2\delta^2/\hbar^2})^{1/2}}, \tag{4}$$

where x_0, p_0, and δ are taken to be real quantities. Superposition of the states given by Eqs. (3) and (4) can give the representation of the single-particle compass state considered in Zurek [1]. The compass state proposed here is given by

$$\Psi(x_1,x_2) = \mathcal{N}[A\psi(x_1)\phi(x_2) + B\phi(x_1)\psi(x_2)], \tag{5}$$

where $\mathcal{N}$ is the normalization constant. It should be mentioned that the nonseparability condition for the wave functions of continuous variables is not fully established. The state in Eq. (5) does not satisfy the separability criterion based on the variance approach [8,9].

From Eq. (5) the correlation function is obtained,

$$c(x_1,a_1,x_2,a_2) = \Psi^\dagger\left(x_1+\frac{a}{2},x_2+\frac{b}{2}\right)\Psi\left(x_1-\frac{a}{2},x_2-\frac{b}{2}\right). \tag{6}$$

The Wigner function, in four-dimensional phase space, can then be defined as

$$W(x_1,p_1;x_2,p_2) = \frac{1}{(2\pi\hbar)^2}\int_{-\infty}^{\infty}\int_{-\infty}^{\infty} c(x_1,a_1,x_2,a_2)e^{i(p_1a+p_2b)/\hbar}da\,db. \tag{7}$$

A lengthy calculation yields

$$W(x_1,p_1;x_2,p_2) = \frac{2\delta^2c|\mathcal{N}|^2}{\pi\hbar^2}e^{-(x_1^2+x_2^2)/\delta^2-(p_1^2+p_2^2)\delta^2/\hbar^2}[W_{D1}+W_{D2} + e^{-x_0^2/2\delta^2-p_0^2\delta^2/2\hbar^2}(W_{C1}+W_{C2})], \tag{8}$$

where, W_{D1}, W_{D2} and W_{C1}, W_{C2} are, respectively, the diagonal and off-diagonal components of the Wigner function. The first diagonal terms can be written as

$$W_{D1} = 2|A|^2\left[e^{-x_0^2/\delta^2-p_0^2\delta^2/\hbar^2}\cosh\left(\frac{2p_0p_2\delta^2}{\hbar^2}\right)\cosh\left(\frac{2x_0x_1}{\delta^2}\right) + e^{-x_0^2/\delta^2}\cosh\left(\frac{2x_0x_1}{\delta^2}\right)\cos\left(\frac{2p_0x_2}{\hbar}\right) + e^{-p_0^2\delta^2/\hbar^2}\cos\left(\frac{2x_0p_1}{\hbar}\right)\cosh\left(\frac{2p_0p_2\delta^2}{\hbar^2}\right) + 2\cos\left(\frac{2p_0x_2}{\hbar}\right)\cos\left(\frac{2x_0p_1}{\hbar}\right)\right]. \tag{9}$$

It can be seen from above that the first three terms containing hyperbolic functions are multiplied by constant Gaussian factors which are bound to be small, in the present mesoscopic context concerned with relatively larger values of x_0 and p_0. Thus only the last term in Eq. (9) becomes dominant in the region between the Gaussians. This term is a purely oscillating term, which can produce a significant amount of interference. The zeros of this term occur at $x_2 = \pm\pi\hbar/4p_0$ and $p_1 = \pm\pi\hbar/4x_0$ from which one can calculate the fundamental area of the tile as $(2\pi\hbar)^2/4x_0p_0$. It should be noted that Eq. (9) has an $|A|^2$ factor and the above calculation does not require any information about entanglement. Indeed one can see sub-Planck structure in this plane even when $|B|=0$. Since this plane has mixed coordinates, i.e., momentum p_1 of particle 1 and position x_2 of particle 2, the structures observed here may not be physically important. The other diagonal term with coefficient $|B|^2$ has similar structure. It ought to be noted that, though W_{C1} and W_{C2} have purely oscillatory terms, they are greatly suppressed as compared to W_{D1} and W_{D2}, for large values of x_0 and p_0. From the discussion so far, one may wonder if it is possible at all to see checkerboard type sub-Planck structures in the x_1p_1 or x_2p_2 plane. The answer to this question can be found by adding the oscillatory terms from W_{D1} and W_{D2},

$$4|A|^2\cos\left(\frac{2p_0x_2}{\hbar}\right)\cos\left(\frac{2x_0p_1}{\hbar}\right) + 4|B|^2\cos\left(\frac{2p_0x_1}{\hbar}\right)\cos\left(\frac{2x_0p_2}{\hbar}\right). \tag{10}$$

From the above, the distance between two zeros in the x_1 direction is again $\pm\pi\hbar/4p_0$ while it is $\pm\pi\hbar/4x_0$ in the p_1 direction. This gives the area of the fundamental tile $a = (2\pi\hbar)^2/4x_0p_0$ in the x_1p_1 plane of particle 1. Similarly, one can find zeros in the x_2 and p_2 directions and obtain the same value of the fundamental area. It should be noted that the fundamental area a, though, does not depend upon A or B. However, both A and B must be simultaneously nonzero in order to have sub-Planck structures in the physical x_1p_1 or

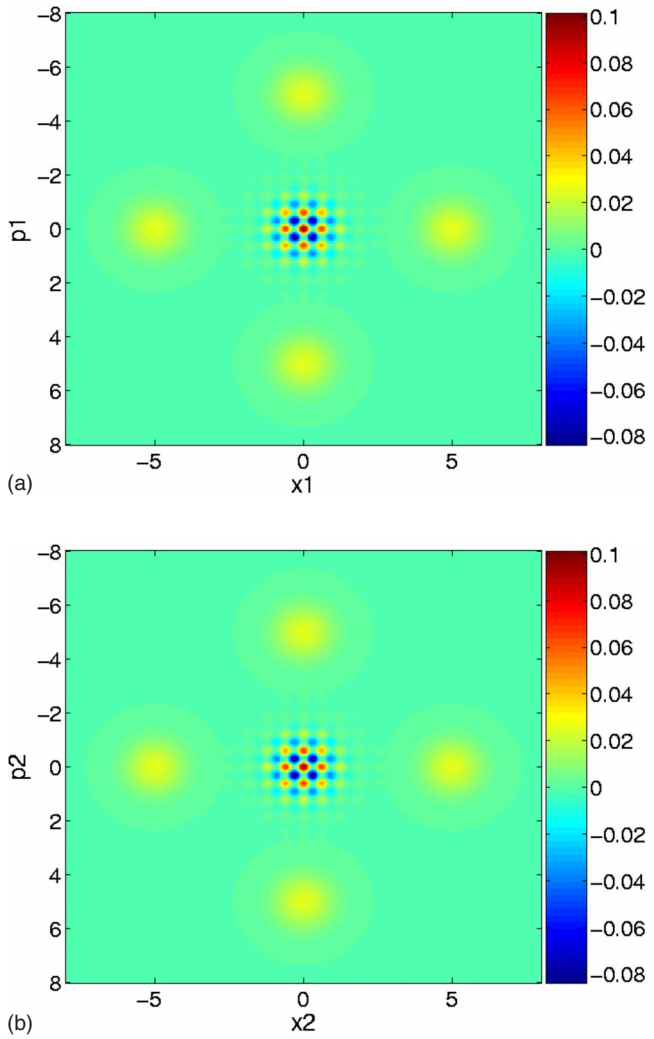

FIG. 1. (Color online) Cross-sectional view of the Wigner function of an entangled wave function with $A_1=A_2=1/\sqrt{2}$ and $B_1=-B_2=1/\sqrt{2}$ in (a) the (x_1p_1) plane, with $x_2=0$, $p_2=0$ and (b) the (x_2p_2) plane with $x_1=0$, $p_1=0$.

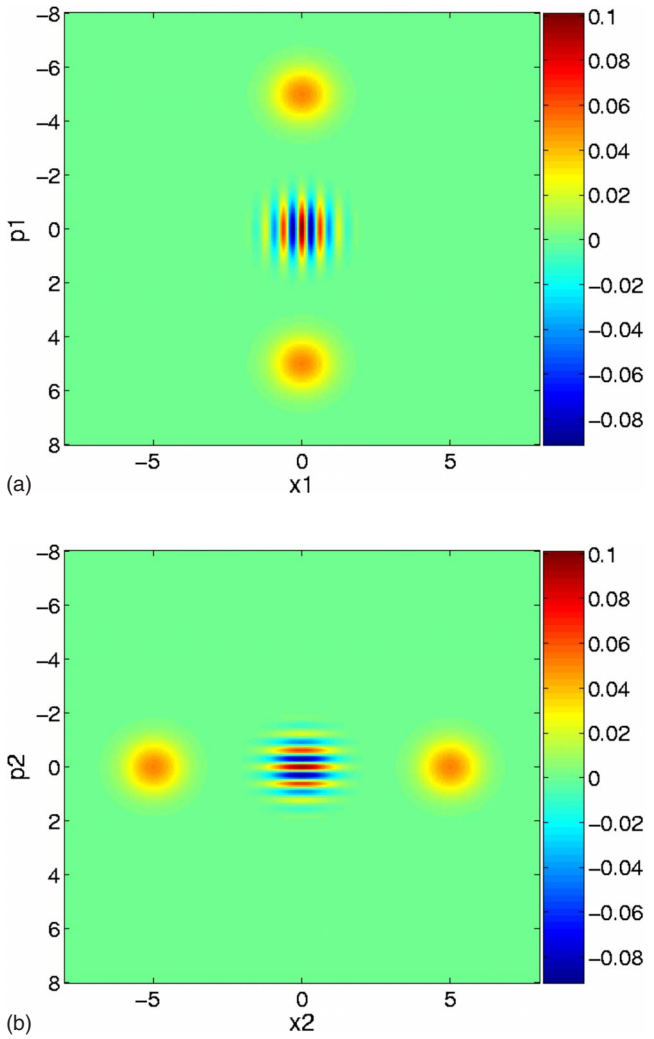

FIG. 2. (Color online) Cross-sectional view of the Wigner function with parameter values as in Fig. 1 except the entanglement has been turned off by setting the parameter $B=0$.

x_2p_2 plane. It is clear that the visibility of the interference patterns depends upon the relative magnitudes of A and B. In Figs. 1 and 2 we have shown plots of the Wigner function [Eq. (8)] in x_1p_1 and x_2p_2 planes. Figure 1 depicts the cross-sectional view of the Wigner function in the x_1p_1 and x_2p_2 planes while A and B are both nonzero. It clearly shows the checkerboard-type pattern with $a \ll \hbar$. The area of the fundamental tile matches a that we have calculated above. These plots look very similar to that in [1], but no oblique sidebands, as seen in [1], are visible in our figure. The oblique sidebands in our case come from the off-diagonal terms W_{C1} and W_{C2}. As seen in Eq. (9) they are multiplied by constant Gaussian factors and their contribution to the Wigner function is strongly suppressed for sufficiently large values of x_0 and p_0. In this sense, we observe a cleaner checkerboard-type pattern using the bipartite compass state.

Figure 2 depicts the case when $B=0$ and all the other parameters are the same as in Fig. 1. No sub-Planck structure is seen here, which confirms our assertion that both A and B must be simultaneously nonzero to have these phase-space structures in the x_1p_1 and x_2p_2 planes. We have chosen $x_0, p_0=5$, in units of $\hbar=1$ and $\delta=1$ in plotting Figs. 1 and 2. The circles indicate the positions of the Gaussians. For the $B=0$ case, only two Gaussians are visible.

The sensitivity of the entangled compass state in Eq. (3) can be studied as follows. Let $D_1(\alpha)$ and $D_2(\beta)$ denote two displacement operators causing the displacement of particle states 1 and 2, by amounts α and β, respectively, to create a perturbed state $|\psi_{\text{per}}\rangle = D_1(\alpha)D_2(\beta)|\psi_c\rangle$. The overlap function $|\langle\psi_c|\psi_{\text{per}}\rangle|^2$ can be found to be

$$\begin{aligned}|\langle\psi_c|\psi_{\text{per}}\rangle|^2 = 16|\mathcal{N}|^4\{&|A|^4\cos^2[x_0(\beta+\beta^*)]\cosh^2[x_0(\alpha^*-\alpha)]\\ &+|B|^4\cos^2[x_0(\beta+\beta^*)]\cosh^2[x_0(\alpha^*-\alpha)]\\ &+2|A|^2|B|^2\cos[x_0(\beta+\beta^*)]\cosh[x_0(\alpha^*-\alpha)]\\ &\times\cos[x_0(\beta+\beta^*)]\cosh[x_0(\alpha^*-\alpha)]\}. \qquad (11)\end{aligned}$$

It is particularly of interest to consider the case when there is an equal shift of both particles, i.e., $\alpha=\beta=isx_0/|x_0|$; the overlap function can then be written as

$$|\langle\psi_c|\psi_{\rm per}\rangle|^2 = 8|\mathcal{N}|^4(|A|^2+|B|^2)^2[1+\cos(4x_0 s)]. \quad (12)$$

Clearly the overlap function becomes minimum, for distinguishable displacement, if $s\sim\pi/(4x_0)$. It must be noted that the states described by Eq. (2) also give the same value of s. For instance, when the particles are untangled, i.e., when either A or B is zero, the value of the minimum distinguishable displacement does not change. However, these kinds of states do not have the checkerboard kind of pattern (as shown in Fig. 2), and consequently they do not provide sensitivity in the precision measurement in all directions of phase space. Thus the entangled state given by Eq. (1) does not improve upon the accuracy provided by the constituent states [Eq. (2)], but it rather provides a sensitivity in all the directions of phase space during a precision measurement.

Next consider the displacement of the compass state given in Refs. [1,2], by amount s_1, the overlap function can be written as

$$\frac{1}{4}[3+4\cos(2x_0 s_1)+\cos(4x_0 s_1)]. \quad (13)$$

This function becomes minimum for $s_1\sim\pi/(2x_0)$. Since x_0 is a parameter that can be fixed by an experiment, both $|\psi\rangle_c$ and the state given in Refs. [1,2] can be used for Heisenberg-limited precision measurements. What we have shown here is that the distinguishable displacement coming from the entangled state is a factor of $1/2$ less than the one found in Ref. [2] when x_0 remains the same. This implies that the same level of accuracy as in a nonentangled compass state can be obtained with $|\psi\rangle_c$ if x_0 is reduced by a factor of $1/2$. Although the entanglement has not increased, the sensitivity of states in Eq. (2), it has given us sensitivity in all directions in phase space. More precision is gained because the states in Eq. (2) are more sensitive than the compass state in Ref. [1]. This is perhaps the most intriguing feature that entanglement brings into the problem. Interestingly, this can also help in increasing the decoherence time of $|\psi\rangle_c$. In a practical situation the interaction time T during which the compass state undergoes perturbation must be much smaller than its lifetime t_d. For example, for a cavity QED system $t_d\sim t_c/2x_0^2$, t_c is the lifetime of the cavity field [4]. Thus, when $x_0\rightarrow x_0/2$, the lifetime t_d of $|\psi\rangle_c$ increases by four times compared to the nonentangled compass state [2], keeping x_0 the same. This would certainly help in satisfying the important condition $T\gg t_d$. With regard to the possibility of experimental realization of the proposed continuous-variable entangled states, we would like to point out two different scenarios, involving cavity QED and its fractional rival in molecular wave packets. In the case of cavity QED, one can start with superposed states after which a 50:50 beam splitter can be applied to achieve entanglement. It needs to be mentioned that superposed cat states have been experimentally realized in cavity QED [10]. In the case of molecular wave packets, generation of cat and superposed cat states has been demonstrated in fractional revival [5]. The procedure to produce entangled states from the above type of state has been recently explained [11]

In conclusion, we have studied the phase-space structures in a bipartite system of entangled superposed coherent states. These structures are shown to originate from entanglement. They are argued to be more robust against decoherence. Furthermore, these structures are cleaner in this case due to the suppression of the sidebands. We have also shown that this kind of compass state may be useful in carrying out precision quantum measurements.

[1] W. H. Zurek, Nature (London) **412**, 712 (2001).

[2] F. Toscano, D. A. R. Dalvit, L. Davidovich, and W. H. Zurek, Phys. Rev. A **73**, 023803 (2006).

[3] Ph. Jacquod, I. Adagideli, and C. W. J. Beenakkar, Phys. Rev. Lett. **89**, 154103 (2002).

[4] G. S. Agarwal and P. K. Pathak, Phys. Rev. A **70**, 053813 (2004).

[5] S. Ghosh, A. Chiruvelli, J. Banerji, and P. K. Panigrahi, Phys. Rev. A **73**, 013411 (2006).

[6] L. Praxmeyer, P. Wasylczyk, C. Radzewicz, and K. Wòdkiewicz, Phys. Rev. Lett. **98**, 063901 (2007).

[7] S. J. van Enk and O. Hirota, Phys. Rev. A **64**, 022313 (2001).

[8] L.-M. Duan, G. Giedke, J. I. Cirac, and P. Zoller, Phys. Rev. Lett. **84**, 2722 (2000); E. Shchukin and W. Vogel, *ibid.* **95**, 230502 (2005).

[9] R. Simon, Phys. Rev. Lett. **84**, 2726 (2000).

[10] M. Brune, E. Hagley, J. Dreyer, X. Maitre, A. Maali, C. Wunderlich, J. M. Raimond, and S. Haroche, Phys. Rev. Lett. **77**, 4887 (1996); J. M. Raimond, M. Brune, and S. Haroche, *ibid.* **79**, 1964 (1997).

[11] E. A. Shapiro, M. Spanner, and M. Y. Ivanov, Phys. Rev. Lett. **91**, 237901 (2003).